Vol. 207: 53–68, 2000 | MARINE ECOLOGY PROGRESS SERIES
Mar Ecol Prog Ser | Published November 22

Formation, degradation, and mass:volume ratios of detritus derived from decaying phytoplankton

P. G. Verity*, S. C. Williams, Y. Hong

Skidaway Institute of Oceanography, 10 Ocean Science Circle, Savannah, Georgia 31411, USA

ABSTRACT: The mass of non-living particulate organic matter, or detritus, often exceeds that of living plankton in pelagic environments; in coastal waters the difference can be 10-fold. Relatively little is known about the dynamics of this pool of organic matter because it has not been previously possible to accurately determine its magnitude. A recent approach utilizing fluorescence microscopy (Verity et al. 1996) provided estimates of the volume of detritus. Here, laboratory experiments were conducted to estimate carbon:volume (C:V) and nitrogen:volume (N:V) conversion ratios of detritus formed by 2 phytoplankton species when incubated in darkness in the presence of bacteria. The volume of detritus was measured directly, along with total particulate organic carbon (POC) and nitrogen (PON), and that contained in the associated phytoplankton and bacterial communities. Detrital carbon and nitrogen were estimated by difference and compared to detrital volume, from which conversion factors were calculated. The physiological state of the bacteria was assessed using a recently developed fluorescent stain and molecular probe protocol (Williams et al. 1998). The 2 phytoplankton cultures were degraded at different rates. At the times of peak bacterial abundances, most of the remaining bulk POC and PON was in the form of bacteria cells. Conversion efficiencies, however, were only 8 to 9% (carbon) and 10 to 11% (nitrogen). The fraction of the bacterial community composed of active cells was inversely related to the C:N ratio of the bulk particulate matter in both cultures, although with different absolute values. C:N ratios of detritus, distinct from surrounding bacteria and phytoplankton, were typically 35 to 50 but varied during the 56 d incubations because bacteria selectively degraded PON compared to POC. C:V and N:V ratios were typically 0.09 to 0.11 and 0.002 to 0.004 pg μm^{-3} in fresh detritus, respectively, and ratios declined as the detritus degraded in the presence of bacteria. Mean C:V and N:V ratios were 0.05 to 0.11 and 0.0014 to 0.0031, respectively. These ratios indicate that detritus derived from phytoplankton cultures contains reduced densities of organic carbon and nitrogen compared to living plankton. They provide the means to directly estimate the carbon and nitrogen content of natural detritus, although the C:V and N:V ratios of cultures need to be compared to those estimated from natural plankton communities.

KEY WORDS: Detritus · Phytoplankton · Bacteria · Carbon:volume · Nitrogen:volume · Physiological state

INTRODUCTION

Particulate organic matter (POM) in the ocean is composed of living and non-living components. In ecological research, the focus is typically on living components because of the primary role of plants in the transformation of dissolved inorganic carbon into organic carbon, and because phytoplankton provide the basis for most food webs in the sea. However, estimates of the mass of non-living POM, or detritus, in the sea is often considered to exceed that of plankton (Smetacek & Hendricksen 1979, Gassmann & Gillbricht 1982, Andersson & Rudehall 1993). A generalized ratio of 10:1 detritus:plankton biomass has been proposed (Pomeroy 1980). Detritus has long been considered a 'problem' in phytoplankton research, because detrital carbon biases the estimates made of phytoplankton carbon from total particulate organic carbon (POC) in

*E-mail: peter@skio.peachnet.edu

field samples. Moreover, relatively unique measures of phytoplankton biomass such as chlorophyll *a* (chl *a*) cannot be used to estimate phytoplankton carbon *in situ* because algal C:chl *a* ratios vary with algal physiological state and recent nutrient and light history (Banse 1977).

Dissolved organic carbon (DOC) concentrations are considerably greater than those of detritus, and transformations between DOC and detritus occur via microbial exopolymers (Decho 1990). Detritus, therefore, exchanges between both living POC stocks and DOC pools, and knowledge of detrital biomass and dynamics would improve our ability to understand material fluxes *in situ*. Early carbon flux models predicted that up to 50% of primary production on continental shelves could pass through detritus and yet also support all the major trophic groups (Pomeroy 1979). More recent data have shown that dissolved organic matter, exopolymers, and detritus can coagulate and aggregate, and thereby influence carbon cycling and vertical export (Alber & Valiela 1994, Mari & Burd 1998). Accordingly, detritus is being explicitly considered in contemporary food web and ecosystem models, e.g. Anderson & Williams (1998), Verity (2000). However, until recently we have lacked the ability to directly quantify detritus in natural communities using units of biogeochemical significance, e.g. carbon, nitrogen.

One method to estimate the mass of detritus is to stain it distinct from living plankton and use confocal microscopy to determine the volume of detritus (Williams et al. 1995, Verity et al. 1996). This approach determines detrital volume directly and is not dependent upon other measurements. Detrital volumes can then be compared to plankton volumes, but the data would be more useful if expressed in units of biogeochemical significance, e.g. carbon or nitrogen. Various processes produce and decompose material contained in detritus, and therefore the ratio of POC and particulate organic nitrogen (PON) to particle volume (V) in detritus may or may not be constant. C:V and N:V ratios in detritus may decrease as bacteria mineralize organic matter, ectoenzymes destabilize detritus, and the microbial food web disrupts the integrity of the detrital material (Biddanda & Pomeroy 1988). But these ratios may also increase as DOC adsorbs onto detritus via exopolymers and is cemented by microbial activities (Khaylov & Finenko 1968, Paerl 1974, Biddanda 1988). It was the goal of this study to investigate variability in C:V and N:V ratios under controlled laboratory conditions. Additionally, because of their central role in the degradation of POM, the physiological status of bacteria in these experiments was assessed using a recently developed fluorescent stain and molecular probe combination (Williams et al. 1998).

MATERIALS AND METHODS

Cultures and sampling. Experiments were conducted using 2 phytoplankton species representing different algal classes. *Cryptomonas* sp. was isolated from the Skidaway River estuary, Georgia, USA. *Gymnodinium* sp., culture #AA-15-3260, was provided by Carolina Biological Supply. Cell dimensions were 8.2 × 9.6 µm for *Cryptomonas* sp., with a mean cell volume of 314.8 μm^{-3}; and 4.5 × 5.0 µm for *Gymnodinium* sp., with a mean cell volume of 47.4 μm^{-3}. Neither culture was axenic, and no attempts were made to alter the associated bacterial communities.

In separate experiments, each species was grown in batch culture using autoclaved f/2 media (Guillard 1975) in 4 l polycarbonate bottles. Cultures were grown at 20°C under a 12:12 h light:dark cycle and ca 200 µEinst m^{-2} s^{-1} provided by cool-white fluorescent lamps. Stock cultures of both species were grown to stationary growth phase, which occurred at similar algal carbon concentrations (20 to 25 mg l^{-1}), before initiating the detritus experiments. While residual nutrients were not measured, they were assumed to be minimal because algal growth had ceased.

At the beginning of each experiment (termed Day 0), the bottles containing the cultures were tightly wrapped in multiple layers of aluminum foil, to simulate a senescent algal bloom decaying below the euphotic zone. In the first experiment with *Cryptomonas* sp., sampling began on Day 1 and continued daily for 1 wk; when microscope observations showed that *Cryptomonas* sp. was not degrading rapidly (see 'Results'), sampling frequency was decreased to twice weekly during Days 7 to 24, and then at ca weekly intervals during Days 24 to 57. In the second experiment with *Gymnodinium* sp., samples were collected from the darkened bottles at weekly intervals over Days 0 to 56. Separate bottles with killed controls (to distinguish biotic from abiotic degradation) were not used because the focus was on detrital mass:volume ratios.

On each date, subsamples were collected to separately determine the following parameters (Fig. 1). Abundance and cell volumes of phytoplankton and bacteria were measured using color image analyzed fluorescence microscopy (Sieracki et al. 1989a,b, Verity et al. 1992, Verity & Sieracki 1993). Bacterial abundance and the proportions of active, inactive, and dead bacteria cells were measured using a newly developed Vital Stain and Probe (VSP) technique (Williams et al. 1998). The volume of detritus was determined microscopically following Verity et al. (1996). Because of their relevance, these 3 protocols are described in partial detail below; for complete information, the reader is referred to the cited literature. In addition, the fol-

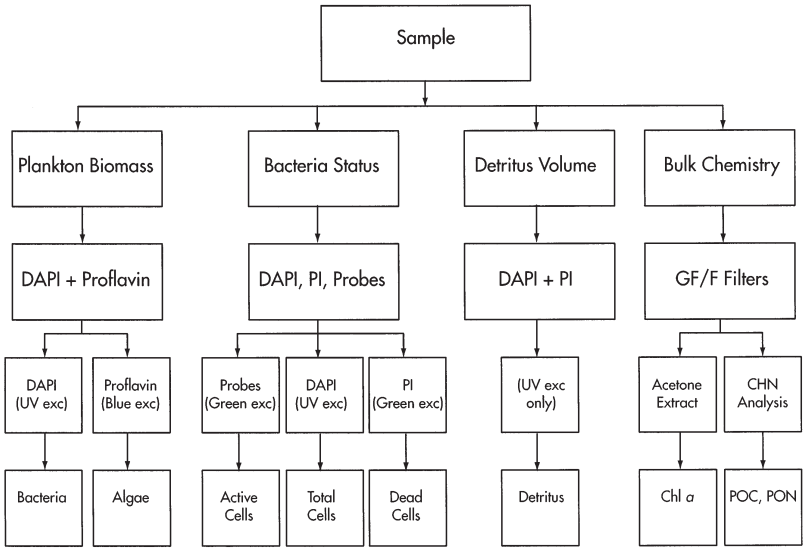

Fig. 1. Flow chart of sample preparation and analysis. See 'Materials and methods' for details

lowing chemical measurements were conducted on Whatman GF/F filtered samples: chl *a* using a Turner Designs Model 10 fluorometer and acetone extractions in the dark (Parsons et al. 1984); and POC and PON using a Fisons NA1500 NCS Series 2 CHNS analyzer and 2.5-Bis(5-tert-butyl-2-benzo-oxazol-2-yl)thiophene (BBOT) standards.

Plankton microscopy. ***Plankton biomass:*** Samples to enumerate and measure phytoplankton cells were initially fixed with glutaraldehyde (0.3% final concentration), stained with DAPI (10 µg ml^{-1} final concentration) for 4 min, then momentarily stained with proflavine (1.4 µg ml^{-1} final concentration), and finally collected on black 0.2 µm Nuclepore filters. Filters were covered with a small drop of low-fluorescence immersion oil and a coverslip, and slides were used immediately or stored frozen at –20°C. Cells were visualized using an Olympus BX-60 fluorescence microscope using 2 Olympus filter sets. Phytoplankton were measured wth a 60× PLANAPO NA 1.4 oil objective and a Narrow Blue filter set (U-M514), with exciter filter BP 470-490, dichroic mirror DM 500, and barrier filter BA 515. Bacteria were measured with a 100X UPLANFL NA 1.3 oil objective and a Wide UV filter set (U-M536), with exciter filter BP 330-385, dichroic mirror DM 400, and barrier filter BA 420. Counting/measuring techniques are described below under 'Image analysis.'

Bacteria physiological status: Bacteria abundance and the proportions of active, inactive, and dead cells were measured using samples prepared according to the VSP technique (Williams et al. 1998). The latter utilizes DAPI as a general cell stain, the membrane viability stain propidium iodide (PI), and 16S rRNA targeted eubacterial-specific (universal) oligonucleotide probes labeled with TRITC (Molecular Probes, Inc., Eugene, OR). Oligonucleotides were labeled by means of a 5′ amino terminus linker or synthesized directly with the appropriate fluor. DAPI was used to enumerate total bacterial cells while PI identified dead cells (Sgorbati et al. 1996, Williams et al. 1998), and 16S rRNA targeted probes identified the metabolically active cells (Giovannoni et al. 1988, Braun-Howland et al. 1992, Lee et al. 1993, Amann et al. 1995). Three unique universally targeted 16S rRNA probes were used in combination to increase probe sensitivity and universality. Probes 'Primer A' (5′-gwattaccgcggckgctg; Lane et al. 1985), 'Primer C' (5′-acgggcggtgtgtrc; Lane et al. 1985), and 'Universal 342' (5′-ctgctgcsycccgtag; Vescio & Nierzwicki-Bauer 1995) were used (ambiguous bases are w = a or u; r = a or g; s = c or g; k = g or u; y = c or u). Preliminary studies demonstrated a detection sensitivity threshold when using 3 such probes of 0.3 fg rRNA cell^{-1} (Hong et al. 1998).

Samples for VSP determination of bacteria were divided into 2 aliquots: 1 sample was placed in 25% (v:v) glycerol for PI:DAPI staining, the remaining sample was preserved with 4% formalin for subsequent probe hybridization. The formalin sample was stained with DAPI (final concentration 3 µg ml^{-1}), and filtered according to standard DAPI procedures (e.g. Verity & Sieracki 1993 and elsewhere). The cells were permeablized in an ethanol:formalin (90:10) for 1 h, and rinsed 3 times with distilled water. One ml of the probe mixture (340 ng ml^{-1}) was applied to each filter containing cells and incubated overnight in a humidified chamber at 37°C. Following hybridization, the filter was washed for 1 h in 3 changes of 1x SET (150 mM NACl, 20 mM Tris-HCl, pH 7.8, 1 mM EDTA) at the hybridization temperature. All of the staining and hybridization procedures were done inside the filter tower to ensure that cells were not lost due to the various washing procedures. The filter was mounted onto a clean glass slide with (50:50) glycerol:1x SET mounting solution and a No. 1 coverslip was applied on top of the filter.

The glycerol aliquot was stained with 3 µg ml^{-1} final concentration of PI and 5 µg ml^{-1} final concentration of DAPI for 30 min and filtered onto a 0.2 µm black polycarbonate filter under low vacuum. The black filter was mounted on a glass slide, and low fluorescence immer-

sion oil was placed on the filter and covered with a No. 1 coverslip. The formalin and glycerol aliquots were both enumerated with an Olympus BX-60 fluorescence microscope equipped with a 100× UPLANFL NA 1.3 oil objective. Overall, 2 Olympus filter cubes were used: a Wide UV filter set (U-M536), with exciter filter BP 330–385, dichroic mirror DM 400, and barrier filter BA 420 (to visualize DAPI-stained total cells); and a Wide Green Filter set (U-M526), with exciter filter BP 510–550, dichroic mirror DM 570, and a barrier filter BA 590 (to visualize probe-positive and PI-positive cells).

Image analysis: Enumeration and sizing of both phytoplankton and bacteria were accomplished using a quasi-automated imaging system designed around an Olympus BX-60 epifluorescent microscope. The heart of the imaging system was similar to that described by Verity & Sieracki (1993), with contemporary upgrades, including a Photonics Science cooled integrating 3-chip color CCD with variable frame rates from 1/10 000 s to 4 min, and an electronic shutter mounted in-line in the microscope lightpath so that the sample was exposed to excitation for only as long as the camera shutter was open. Analysis of an image with 60 cells required 2 s. The computer could automatically select random locations on the slide and return to each location ± 1 µm. The commercial driver software (Image Pro Plus v3.0) was customized so that the entire process (moving to a given location, focusing, opening an electronic shutter, grabbing an image, closing the shutter, and moving to a new location) was automated and computer-controlled. A minimum of 200 phytoplankton cells (Verity et al. 1992), and 20 image fields of bacteria (typically 1000 cells) were measured. Data were automatically exported into spreadsheets, and every cell in an image was uniquely identified for post-measurement visual confirmation. Images of individual phytoplankton and bacteria cells were automatically thresholded using the second derivative method (Sieracki et al. 1989a). Cell biovolume measurements (Sieracki et al. 1989b, Verity & Sieracki 1993) were converted to carbon/nitrogen biomass using empirical equations relating carbon/nitrogen density to cell size of bacteria (Kroer 1994) and phytoplankton (Verity et al. 1992).

Determination of detritus volume. Detritus and plankton in each sample were selectively labelled using sequential application of glutaraldehyde and the fluorescent stains PI and DAPI (Williams et al. 1995). Ten ml samples were stained for 5 min with 450 µl of PI (stock solution: 1 mg PI in 100 ml of phosphate-buffered saline [10^{-3} M, pH 7.2]), and then for 1 min with 300 µl of DAPI [stock solution: 5 mg DAPI in 1000 ml distilled water]. Samples were then concentrated on 0.2 µm black Nuclepore filters. Under wide-band UV excitation (same microscope and filter set as described in 'Image analysis' above), PI in the presence of glutaraldehyde stained detritus red, while DAPI stained it yellow; combined they produced a deep orange color. The brilliant blue/white fluorescence of DNA associated with bacteria and the nuclei of larger plankton, and induced by DAPI, was spectrally distinct and much brighter than detritus. PI stained the cytoplasm of living plankton cells a light pink, very similar to the color associated with the autofluorescence of chlorophyll under UV excitation, so that living cells could be discriminated from detritus. As with most fluorescent stains, it is essential to match stains with appropriate microscope filter sets, so that the excitation and emission characteristics yield the desired visual effects, e.g. cell/particle discrimination. Likewise, protocol efficiency is enhanced when matched with light-sensitive, high-resolution, true-color cameras (e.g. Verity & Sieracki 1993, Shopov et al. 2000).

The volume of detritus collected on the filters was then determined using digital confocal microscopy (Verity et al. 1996). Basically this method carves a 3D spatial volume into a stack of 2D images, and then determines the volume of material within. Briefly, the image analysis software also controlled a *z*-axis motorized stage on the BX-60 microscope. The microscope operator randomly selected a field of view, and set the upper and lower focal planes which comprised the top and bottom 2D images, or optical slices, of the mass of detritus and plankton. Software then drove the *z*-axis motorized stage so that the microscope automatically focused on the top of the detritus in the field of view, the shutter opened electronically (i.e. no vibration), the CCD grabbed an image (an 'optical slice') during the period when the CCD shutter was open, (e.g. 1/30 s), the electronic shutter closed, the motorized microscope stage moved down an exact prescribed amount so that a new 'slice' was in focus, and the procedure was repeated until the surface of the filter was reached. The distance between slices is determined from the numerical aperture and magnification of the microscope objective; at 40× this interslice distance was 1.0 µm.

In the original description of this method (Verity et al. 1996), the stack of 2D images was subsequently deconvolved using a nearest neighbor algorithm. This process compared the distribution of light in each plane of focus with that from the planes immediately above and below, to remove the out-of-focus haze which is an unavoidable by-product of image formation in microscopy. The result was a stack of 2D images, each perfectly in focus and separated by exact known amounts. These image stacks were then relayed to a Silicon Graphics workstation, which interpolated between the 2D image planes and rendered the original volume in 3D, e.g. a plankton cell could be visualized in 3D.

Here, it was not necessary to actually visualize the detritus, but instead only to determine the number and size of the voxels (3D pixels) which corresponded to detritus. The operator used the pink of cytoplasm and blue/white of DNA to distinguish living cells from orange detritus. The *x*/*y* dimensions of each 2D pixel were known directly from the microscope calibrations, and the z-dimension was set by the operator, e.g. 1.0 µm, so the volume corresponding to detritus was calculated directly from each stack of images. It was determined empirically that measurements of the volume of detritus in 20 fields of view was sufficient to stabilize the variance in estimating the volume on the entire filter. Analysis of triplicate filters yielded a coefficient of variation of 8%.

Estimating detrital POC/PON from volume. The carbon and nitrogen content of detritus was calculated as the difference between total combusted POC/PON and that calculated to be contained in bacteria and phytoplankton. All bacteria were retained by the 0.2 µm Nuclepore image analysis filters, but not all the bacteria captured on the image analysis filters were also retained by the CHN filters. This was empirically corrected by enumerating bacteria in whole water samples prior to filtering the POC/PON samples, and again in the filtrate. Tests showed that virtually no detrital particles passed the Whatman GF/F filters which could be subsequently captured on the image analysis Nuclepore filters. The calculated detrital POC and PON from each sample was then compared to the measured volume of detritus in that sample to determine the detrital-carbon: volume and nitrogen:volume ratios for each sample.

Modeling POC and PON degradation. A multi-G model was utilized to describe the degradation of POM (Berner 1980). This approach assumes that organic matter occurs as multiple fractions which degrade at separate rates that can be described by first order exponential decay constants. For simplicity, this process was modeled here as comprising 2 phases:

$$C(t) = (a_1 e^{-b_1 t}) + (a_2 e^{-b_2 t}) + c \quad (1)$$

where $C(t)$ is the POC or PON concentration (mg l^{-1}) at time t; a_1 is the concentration of POC or PON (mg l^{-1}) in the more labile fraction at time t_0; a_2 is the concentration of POC or PON (mg l^{-1}) in the more refractory fraction at time t_0; b_1 is the decay constant (d^{-1}) of the labile fraction; b_2 is the decay constant (d^{-1}) of the refractory fraction; and c is the residual amount (mg l^{-1}).

The data were also fit to a single phase exponential decay model:

$$C(t) = C(0)e^{-kt} \quad (2)$$

where $C(t)$ is the POC or PON concentration (mg l^{-1}) at time t, $C(0)$ is the POC or PON concentration (mg l^{-1}) at time t_0, and k is the first order decay constant. The purpose of this model was to estimate the mean half-life of total POC and PON in the experimental incubations. When k is expressed in natural log units:

$$T_{½} = \ln 2/k \quad (3)$$

where $T_{½}$ is the half-life in days.

The data were fitted with the MacCurveFit statistical program (v 1.5, Kevin Raner Software), using the quasi-Newton method of curve-fitting and the least squares criterion to determine goodness-of-fit.

RESULTS

Cryptomonas sp.

Initial bulk POC and PON concentrations were ca 20 and 4 mg l^{-1}, respectively (Fig. 2A,B). These declined at similar relative rates for the first 14 d, after which POC became relatively conserved in the particulate matter.

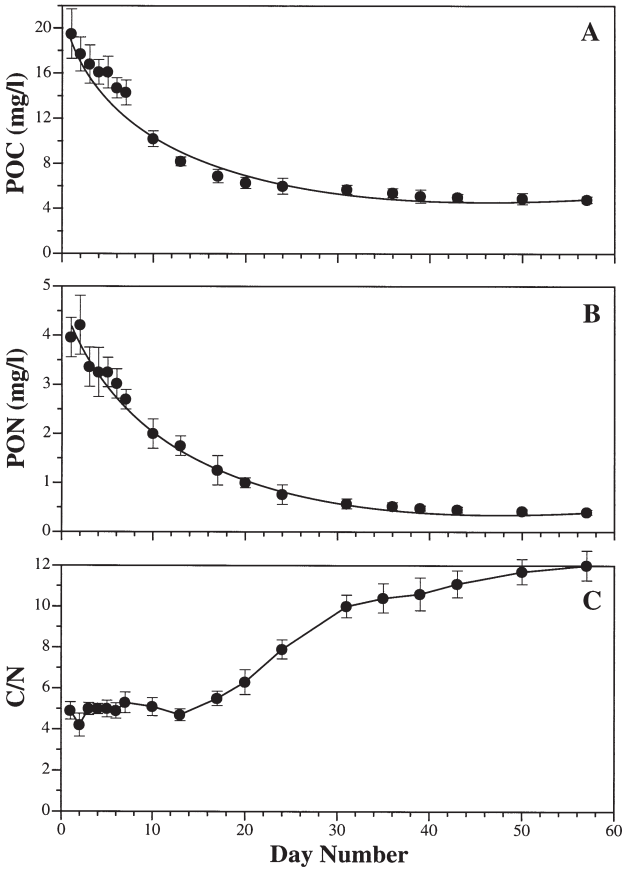

Fig. 2. Changes in (A) bulk particulate organic carbon (POC), (B) particulate organic nitrogen (PON), and (C) the derived C:N ratio during the *Cryptomonas* sp. degradation experiment. Error bars represent SD of replicate subsamples. Curves (A,B) represent data fit to the dual phase degradation model. Parameter estimates in Table 1

Table 1. Model parameters fit ($\bar{x}$ ± SD) to data from the *Cryptomonas* sp. degradation experiment

Parameter	POC	PON
a_1 (mg l^{-1})	16.3 ± 1.5	3.9 ± 0.1
a_2 (mg l^{-1})	3.5 ± 1.6	0.3 ± 0.1
b_1 (d^{-1})	0.09 ± 0.01	0.09 ± 0.01
b_2 (d^{-1})	0.007 ± 0.001	0.01 ± 0.004
c (mg l^{-1})	4.8 ± 2.6	0.4 ± 0.3
$T_{1/2}$ (d^{-1})	27.7	16.9

The C:N ratio (w:w) of POM was stable at 5 to 6 over the initial 2 wk and then climbed steadily to 12 at the end of the experiment (Fig. 2C). The dual-phase degradation model matched both POC and PON data well (Fig. 2A,B). Model parameters (Table 1) indicated that more rapidly degradable or leachable fractions comprised 82% and 92% of POC and PON, respectively. The rate constants predicted that 60 to 65% of the POC and PON in the more labile fraction was lost within 10 d. The rate constants for the less labile fractions suggest an order of magnitude slower leaching or degradation of this POC and PON. Experimental data fit to the single phase exponential model predict half-lives of 28 and 17 d, respectively (Table 1). After 56 d, 25 and 10% of the original POC and PON, respectively, remained (Fig. 2).

Chl *a* was ca constant over the first 7 d at 560 to 600 µg l^{-1}, rapidly declined to 177 µg l^{-1} on Day 17, and slowly decreased to <3 µg l^{-1} by Day 57 (Fig. 3A). The C:chl *a* ratio was comparatively constant at 29 to 40 during the first 17 d, increased to 68 by Day 36, and continued to increase rapidly to 1846 by the end of the experiment (Fig. 3B). The N:chl *a* ratio followed a similar trend, with stable values of 5 to 6 during the first 3 wk and then rapid increases to 140–154 during the eighth week (Fig. 3B).

Total bacteria concentrations increased from 0.8 to 2.6×10^8 cells ml^{-1}; most of the increase occurred during the first 17 d (Fig. 4A). The bacterial communities consisted primarily of rods and cocci, with rare short filaments. The fraction of bacteria cells which were metabolically active was 80 to 90% during the first 5 wk and declined to 70% during the last weeks (Fig. 4B). The fraction of dead cells (compromised membranes) was very small (1 to 8%) throughout the experiment (Fig. 4B). By difference, inactive cells (low

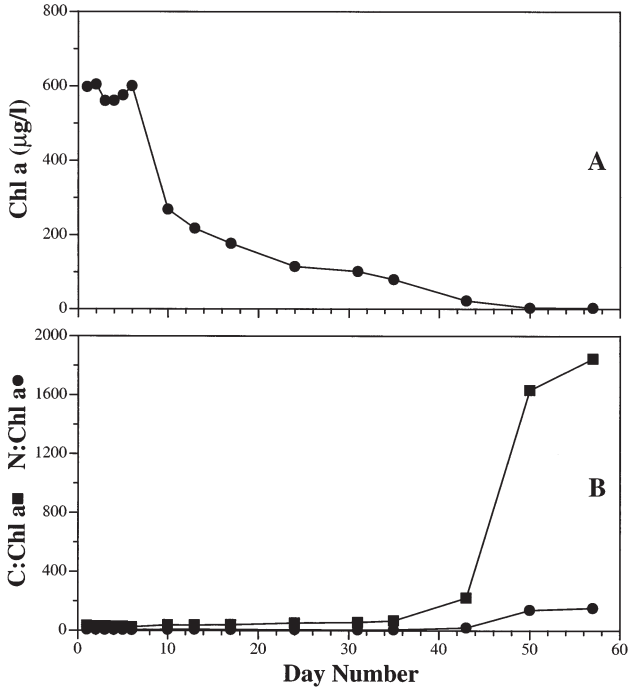

Fig. 3. Changes in (A) chlorophyll *a* concentration, and (B) derived POC:chl (■) and PON:chl (●) ratios during the *Cryptomonas* sp. degradation experiment

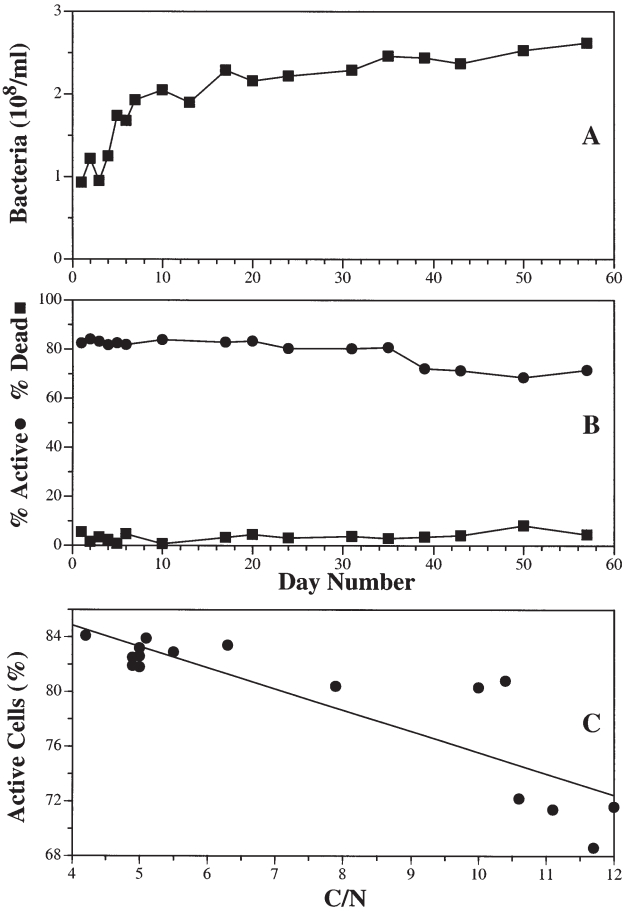

Fig. 4. Changes in (A) concentration of total DAPI-stained bacteria; (B) metabolically active (●) and dead (■) cells as determined by the VSP method (see 'Materials and methods' for details); and (C) linear regression fit to data on active cells versus bulk C:N ratios during the *Cryptomonas* sp. degradation experiment. % active cells = –1.6 (C:N) + 91.1, r^2 = 0.75

rRNA but with functional membranes) represented 5 to 10% during the first 17 d, 10 to 15% during Days 20 to 36, and 20 to 25% during Days 39 to 57. The metabolically active fraction was inversely related to the C:N of the particulate matter (Fig. 4C). The linear regression model explained 75% of the variance in activity and predicted that >90% of the bacterial community would be metabolically active when particulate matter was highly nitrogenous.

At the beginning of the experiment, almost all of the POC was in the form of *Cryptomonas* sp. cells (Fig. 5A). Concurrent with declines in bulk POC, *Cryptomonas* sp. lost carbon even faster, and individual cells could not be discriminated after Day 36. Bacterial carbon was initially 1.7 mg l^{-1} and gradually increased to 3.5 mg l^{-1} at the end of the experiment (Fig. 5A). Detrital carbon was initially unmeasurable and increased steadily to 2.7 mg l^{-1} by Days 31 to 36 (Fig. 5A). Thicknesses of detrital particles and aggregates derived from *Cryptomonas* sp., using the present method of concentration on Nuclepore filters, ranged from 1 to 15 µm, with a mean thickness of 9 µm (data not shown). Expressing the same data in relative terms, *Cryptomonas* sp. initially comprised >90% of total POC, and declined to 0% during Days 7 to 39 (Fig. 5B). Bacteria was initially 8 to 10% of total POC, and increased to 70% by the end of the experiment. Carbon in the form of detritus increased from 0% on Day 6 to 50% of total POC by Days 36 to 39, and then declined to 30% by the end of the experiment.

Total PON was initially dominated by *Cryptomonas* sp. (3.8 to 3.9 mg l^{-1}), and total PON declined concomitantly with algal nitrogen until individual cells could not be recognized after Day 36 (Fig. 6A). Bacterial PON increased from 0.25 to 0.5 mg l^{-1} by the middle of the study and then declined to 0.4 mg l^{-1} (Fig. 6A). Detrital PON was low (0 to 0.1 mg l^{-1}) throughout the experiment. In relative terms, *Cryptomonas* sp. initially represented 95% of total PON, and algal nitrogen declined steadily to 0% by Day 43 (Fig. 6B). Unlike POC, bacterial PON rapidly increased throughout the experiment, from 6 to 85%. Detrital PON increased from 0% on Day 13 to 16% on Day 43, and then declined back to 10% by Day 57.

The carbon:volume (C:V) ratios of detritus derived from *Cryptomonas* sp. (Table 2) were 0.09 to 0.10 pg C $µm^{-3}$ during the first days in which significant detritus could be recognized (Days 13 to 17). Detrital C:V ratios were 0.04 to 0.08 pg C $µm^{-3}$ until Day 36 and then declined to 0.02 pg C $µm^{-3}$. The mean (n = 10) was 0.051 ±

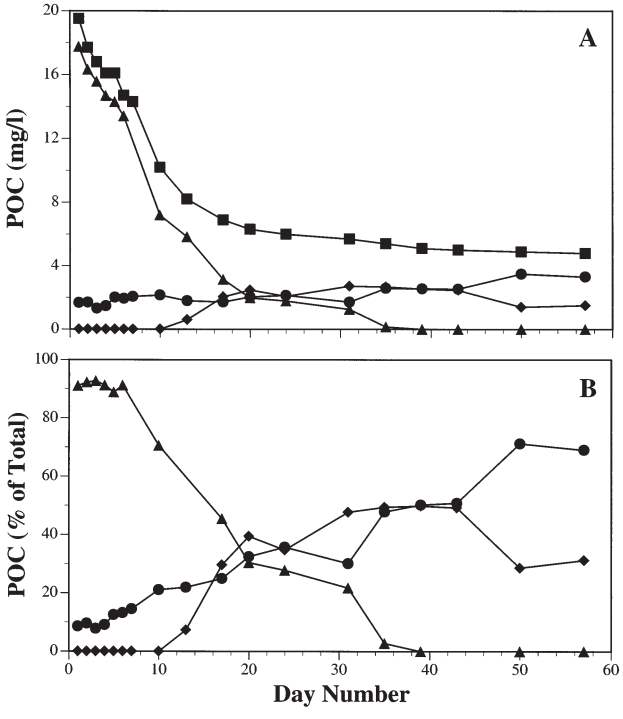

Fig. 5. (A) Changes in bulk POC (■), and in POC contained in bacteria cells (●), in algal cells (▲), and in detritus (◆) during the *Cryptomonas* sp. degradation experiment. (B) Changes in the percentage of POC contained in bacteria cells (●), in algal cells (▲), and in detritus (◆) during the same experiment

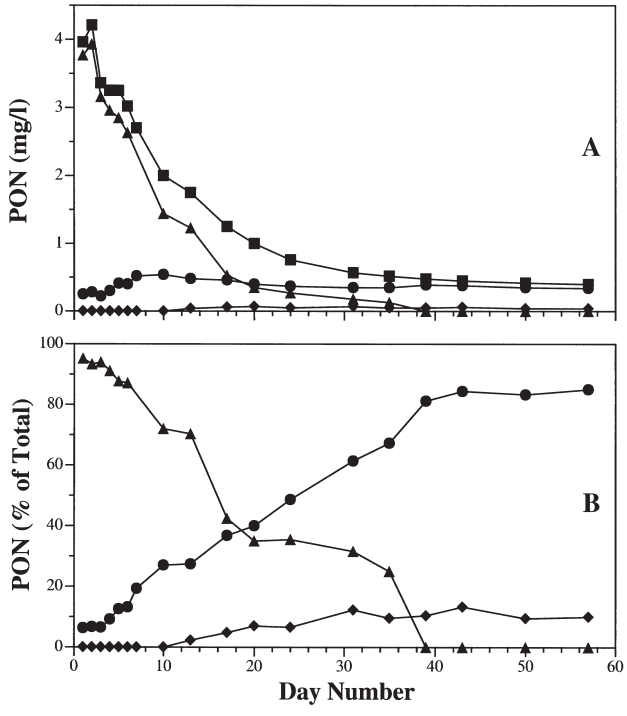

Fig. 6. (A) Changes in bulk PON (■), and in PON contained in bacteria cells (●), in algal cells (▲), and in detritus (◆) during the *Cryptomonas* sp. degradation experiment. (B) Changes in the percentage of PON contained in bacteria cells (●), in algal cells (▲), and in detritus (◆) during the same experiment

Table 2. Detrital carbon:volume (Det C:V) and nitrogen:volume (Det N:V) ratios (pg μm^{-3}) ($\bar{x} \pm SD$), bulk particulate C:N ratios, and detrital C:N ratios during the *Cryptomonas* sp. degradation experiment

Day	Det C:V	Det N:V	Bulk C:N	Det C:N
1	–	–	4.92	–
2	–	–	4.20	–
3	–	–	5.00	–
4	–	–	4.95	–
5	–	–	4.95	–
6	–	–	4.87	–
7	–	–	5.30	–
10	–	–	5.10	–
13	0.096 ± 0.017	0.0035 ± 0.0005	4.69	27.0
17	0.094 ± 0.018	0.0028 ± 0.0007	5.52	34.0
20	0.079 ± 0.009	0.0022 ± 0.0003	6.30	35.5
24	0.050 ± 0.007	0.0012 ± 0.0003	7.89	41.6
31	0.057 ± 0.004	0.0015 ± 0.0002	10.00	38.9
36	0.045 ± 0.005	0.0008 ± 0.0002	10.38	53.4
39	0.031 ± 0.004	0.0006 ± 0.0002	10.62	50.8
43	0.026 ± 0.002	0.0006 ± 0.0002	11.11	41.0
50	0.015 ± 0.003	0.0004 ± 0.0001	11.67	35.0
57	0.018 ± 0.003	0.0005 ± 0.0002	12.00	37.5

0.030 pg C μm^{-3}. Detrital nitrogen:volume (N:V) ratios were much more variable (Table 2): initially high at 0.0035 pg N μm^{-3} (Day 13), N:V ratios decreased quickly to 0.0012 to 0.0015 pg N μm^{-3} (Days 24 to 31), and eventually 0.0004–0.0005 pg N μm^{-3} at the end of the experiment. The mean (n = 10) was 0.0014 ± 0.0011 pg N μm^{-3}. The initial C:N ratio of detritus (27) was 5 to 6 times higher than bulk POM (4 to 5) (Table 2). Detrital material became further enriched in carbon relative to nitrogen, with C:N ratios of 34 to 54 during Days 17 to 57. The mean C:N ratio of detritus (n = 10) was 39.5 ± 7.8.

Gymnodinium sp.

The total POC and PON in the *Gymnodinium* sp. culture was initially 25 and 4.5 mg l^{-1}, respectively (Fig. 7A,B). Carbon and nitrogen were lost from particulate matter roughly equally during the first 14 d, after which nitrogen losses accelerated. After 56 d, ca 3 and 0.2 mg l^{-1} remained of POC and PON, respectively. C:N ratios of total POM (Fig. 7C) were 5.6 to 6.9 during the first 14 d, and then increased steadily to 19.8 (Day 56). The dual-phase degradation model matched both POC and PON data well (Fig. 7A,B). Model parameters (Table 3) indicated that more rapidly degradable fractions comprised 94 and 54% of POC and PON, respectively. The rate constants predicted that 45 to 47% of the POC and PON in the rapidly degradable fraction was lost within 10 d. The rate constants for the less labile fractions suggest an order of magnitude slower leaching or degradation of POC but similar losses of PON. Experimental data fit to the single phase exponential model predict half-lives of 18 and 10 d, respectively (Table 3). After 56 d, 12 and 2% of the original POC and PON, respectively, remained undegraded (Fig. 7).

Compared to *Cryptomonas* sp., chl *a* content of *Gymnodinium* sp. declined quickly with incubation in darkness (Fig. 8A), from 100 to 2.6 µg l^{-1} during Days 0 to 28, and then to zero. C:chl *a* and N:chl *a* ratios in *Gymnodinium* sp. (Fig. 8B,C) were higher than in *Cryptomonas* sp. C:chl *a* ratios increased from 243 to 2288, while N:chl *a* ratios were 35 to 226.

Total bacteria cells were 2.4 to 2.7 × 10^8 cells ml^{-1} during Days 0 to 14, increased to 2.9 to 3.3 × 10^8 cells ml^{-1} (Days 21 to 42), and then declined to 1.1 to 1.2 × 10^8 cells ml^{-1} (Days 49 to 56)

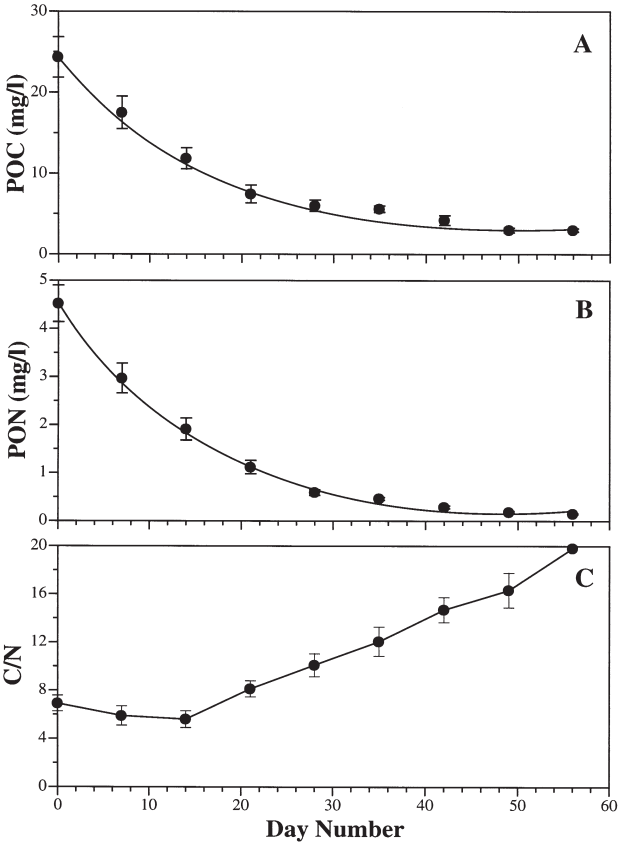

Fig. 7. (A) Changes in bulk POC, (B) PON, and (C) the derived C:N ratio during the *Gymnodinium* sp. degradation experiment. Error bars represent SD of replicate subsamples. Curves (A,B) represent data fit to the dual phase degradation model. Parameter estimates in Table 3

Table 3. Model parameters fit ($\bar{x}$ ± SD) to data from the *Gymnodinium* sp. degradation experiment

Parameter	POC	PON
a_1 (mg l^{-1})	23.1 ± 4.1	2.5 ± 1.3
a_2 (mg l^{-1})	1.5 ± 0.4	2.1 ± 0.7
b_1 (d^{-1})	0.06 ± 0.02	0.07 ± 0.05
b_2 (d^{-1})	0.007 ± 0.004	0.07 ± 0.04
c (mg l^{-1})	3.0 ± 1.8	0.1 ± 0.1
$T_{1/2}$ (d)	18.4	10.1

(Fig. 9A). The bacterial community consisted of both rods and cocci, and were not obviously different in cell morphology from the *Cryptomonas* sp. bacterial community. Unlike *Cryptomonas* sp., however, smaller percentages of bacteria cells contained sufficient rRNA to be considered metabolically active (see 'Discussion'). Initially, 26 to 28% of total cells were active, which declined to 7–9% by Day 56 (Fig. 9B). Conversely, 10 to 12% of cells were initially dead (compromised membranes), which declined to 3–4%. By comparison, the proportion of cells which were inactive but not dead increased from 62–63% early in the experiment to 88–90% by Days 49 to 56. As with *Cryptomonas* sp., the metabolically active fraction was inversely related to the C:N of the particulate matter (Fig. 9C). The linear regression model explained 82% of the variance in activity and, unlike *Cryptomonas* sp., predicted only 33% of the bacterial community would be metabolically active when particulate matter derived from *Gymnodinium* sp. was highly nitrogenous.

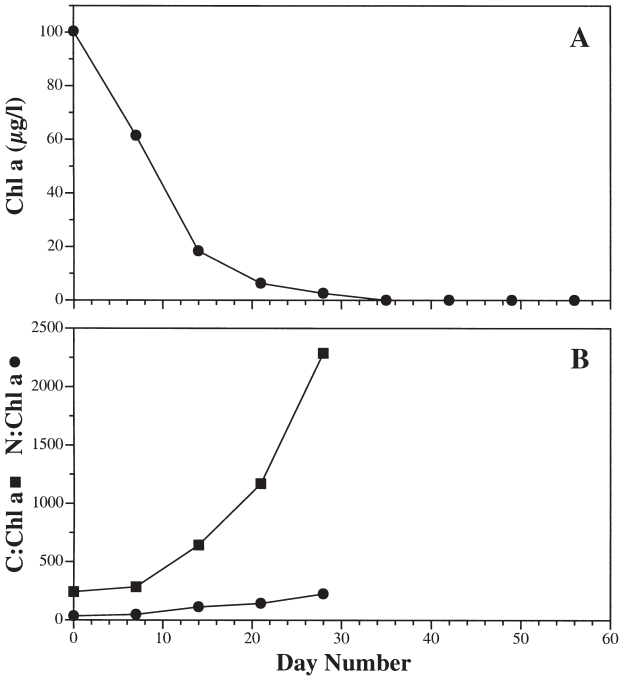

Fig. 8. (A) Changes in chlorophyll *a* concentration, and (B) derived POC:chl (■) and PON:chl (●) ratios during the *Gymnodinium* sp. degradation experiment

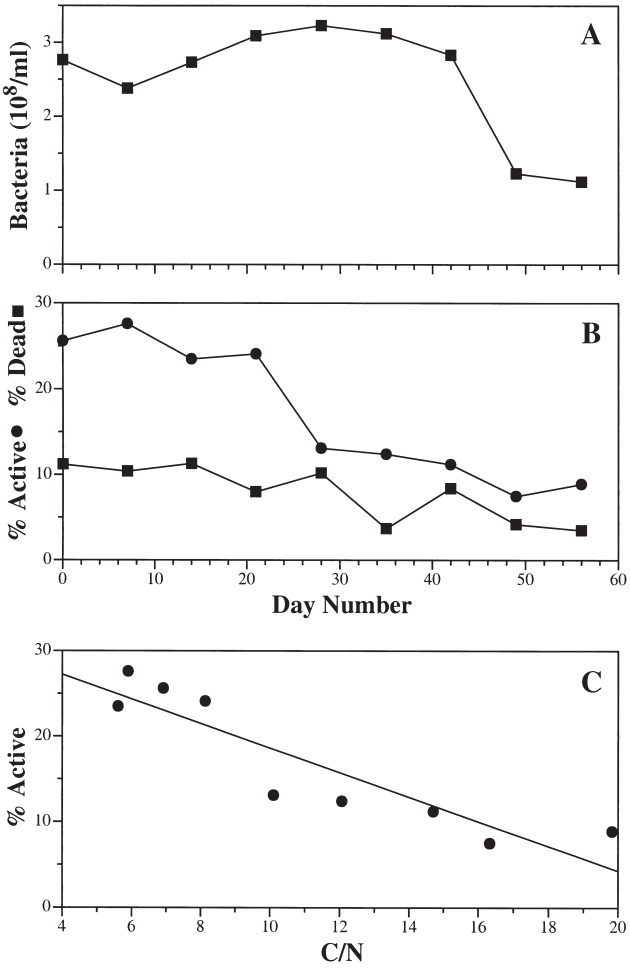

Fig. 9. (A) Changes in concentration of total DAPI-stained bacteria, (B) metabolically active (●) and dead (■) cells as determined by the VSP method (see 'Materials and methods' for details), and (C) linear regression fit to data on active cells versus bulk C:N ratios during the *Gymnodinium* sp. degradation experiment. % active cells = –1.4 (C:N) + 33.0, r^2 = 0.82

As with *Cryptomonas* sp., most of the total POC was contained in *Gymnodinium* sp. for the first 2 wk, even as algal POC declined from 23 to 8 mg l^{-1} (Day 14) to 0 mg l^{-1} (Day 35) (Fig. 10A). Bacterial POC increased from 2 to 3 mg l^{-1} (Days 21 to 28) and then declined to 1 mg l^{-1} (Day 56). Detrital POC was unmeasurable during Days 0 to 14, increased to 3 mg l^{-1} (Day 42), and declined slightly to 2.5 mg l^{-1} by Day 56. Thickness of individual detrital particles derived from *Gymnodinium* sp., using the present method of concentration on Nuclepore filters, ranged from 1 to 11 µm, with a mean thickness of 7 µm (data not shown). In relative terms,

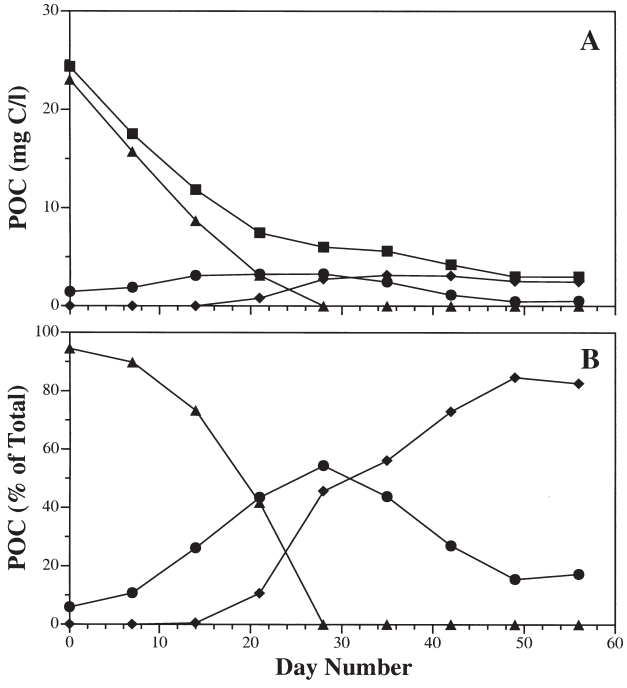

Fig. 10. (A) Changes in bulk POC (■), and in POC contained in bacteria cells (●), in algal cells (▲), and in detritus (◆) during the *Gymnodinium* sp. degradation experiment. (B) Changes in the percentage of POC contained in bacteria cells (●), in algal cells (▲), and in detritus (◆) during the same experiment

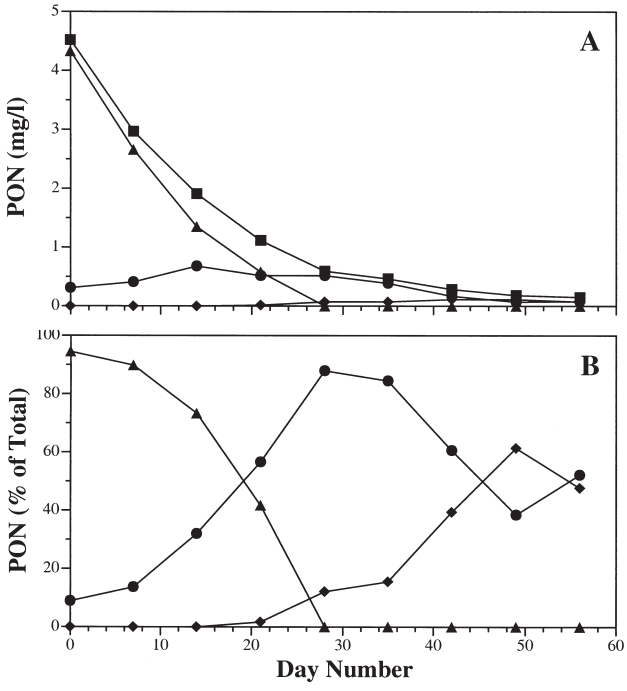

Fig. 11. (A) Changes in bulk PON (■), and in PON contained in bacteria cells (●), in algal cells (▲), and in detritus (◆) during the *Gymnodinium* sp. degradation experiment. (B) Changes in the percentage of PON contained in bacteria cells (●), in algal cells (▲), and in detritus (◆) during the same experiment

Gymnodinium sp. initially represented 96% of total POC and decreased rapidly to 0% (Day 28) (Fig. 10B). Bacterial POC was initially <10% of total POC, increased steadily to 55% (Day 28), and then declined to 15–18% by the end of the experiment. Detrital POC increased steadily from 0% (Days 0 to 14) to 82–85% (Days 49–56).

Gymnodinium sp. PON (Fig. 11A) declined similar to POC, from 3.3 to 0.4 mg l^{-1} (Day 21) to 0 mg l^{-1} (Days 28 to 56). Bacterial PON increased slightly from 0.3 to 0.7 mg l^{-1} (Day 14), and then declined steadily to 0.1 mg l^{-1} on Day 56. Detrital PON was unmeasurable during Days 0 to 14 but increased gradually to 0.2 mg l^{-1}. In relative terms, *Gymnodinium* sp. was initially 95% of the total PON (Fig. 11B) and declined to 0% (Day 28) similar to % POC. The fraction of PON contained within bacteria increased rapidly from 10 to 88% (Day 28), and then gradually decreased to 38–52% (Days 49 to 56). Detritus represented 0% during Days 0 to 14, and increased gradually to 38–52% by the end.

The C:V ratios of detritus derived from *Gymnodinium* sp. (Table 4) were quite constant at 0.097 to 112 pg C μm^{-3} during the 6 wk in which significant detritus could be recognized. The mean (n = 6) was 0.105 ± 0.006 pg C μm^{-3}. Detrital N:V ratios generally increased gradually during the experiment from 0.0032 to 0.0044 pg N μm^{-3}, with a decrease in the final sample (Table 4). The mean (n = 6) was 0.0033 ± 0.0007 pg N μm^{-3}. The C:N ratios of detritus were considerably higher than that of the total POM in each sample (Table 4). C:N ratios of detritus were highest after 5 wk of degradation, with a mean (n = 6) of 32.8 ± 7.6.

DISCUSSION

Because of its broad range of particle sizes and diversity of biochemical composition, 'detritus' is operationally defined. It can include particles ranging from the smallest exopolymers, equivalent to colloids (Decho 1990), to the largest organic aggregates and marine snow (Alldredge 1998). Detritus can be morphous or amorphous in shape, and be derived from aquatic intertidal, terrestrial, or sedimentary sources (e.g. Alber & Valiela 1994). It can be highly labile or very refractory, protein- or carbohydrate-rich, and vary in composition according to particle origin, size, and age (Gordon 1970, Otsuki & Hanya 1972, Newell et al. 1981, Rice 1982, Osinga et al. 1997). This variability can potentially influence the specificity of the protocol used to distinguish detritus (for discussion, see Williams et al. 1995, Schumann & Rentsch 1998). Detritus is defined here as non-living POM which stains using the procedure of Williams et al. (1995) and is collected on 0.2 µm Nuclepore filters. It is unknown the extent to

Table 4. Detrital carbon:volume (Det C:V) and nitrogen:volume (Det N:V) ratios (pg μm^{-3}) ($\bar{x} \pm$ SD), bulk particulate C:N ratios, and detrital C:N ratios during the *Gymnodinium* sp. degradation experiment

Day	Det C:V	Det N:V	Bulk C:N	Det C:N
0	–	–	6.92	–
7	–	–	5.90	–
14	–	–	5.61	–
21	0.0972 ± 0.020	0.0032 ± 0.0004	8.14	30.3
28	0.1103 ± 0.015	0.0029 ± 0.0005	10.11	38.2
35	0.1118 ± 0.019	0.0026 ± 0.0003	12.07	43.8
42	0.1101 ± 0.014	0.0040 ± 0.0005	14.71	27.5
49	0.0990 ± 0.018	0.0044 ± 0.0006	16.33	22.5
56	0.1031 ± 0.011	0.0030 ± 0.0005	19.83	34.4

which this definition incorporates transparent exopolymeric particles (TEP: Alldredge et al. 1993, Mari & Burd 1998), although it seems likely that there is some overlap.

Detritus serves a central role in most if not all aquatic ecosystems, as it influences or is influenced by microbial activities, nutrient supply rates and ratios, energy and material flows through food webs, particle biogeochemistry, water column optics, and sediment-water exchanges (for review, see Roman & Tenore 1984). During the past 3 decades, several methodological approaches have been used in attempts to quantify detritus and changes in its pool sizes over time, including light microscopy of untreated samples (Kane 1967); histochemical staining (Gordon 1970, Passow & Alldredge 1994); fluorescence microscopy (Mostajir et al. 1995a,b, Schumann & Rentsch 1998); particle counters combined with microscopy (Bode et al. 1994, Schumann & Rentsch 1998); bulk chemistry combined with microscopy (Smetacek 1980, Newell et al. 1981); and radio-labelling, with or without microscopy (Biddanda 1988, Biddanda & Pomeroy 1988, Pett 1989). These procedures used microscopy to directly enumerate detritus particles, to assess co-occurring plankton communities, or both. However, none were able to directly and rapidly measure the volume of detritus exclusive of plankton in aquatic samples.

Historically, 2 major problems have complicated efforts to directly quantify the volume of detritus in a water sample using microscopy. The first was to segregate detritus as distinct from living plankton, and the second was to determine the depth (thickness) of detritus collected on a sample platform, e.g. glass slide. One way to circumvent the first limitation is selective staining with fluorochromes (Williams et al. 1995). The second problem has proven more intractable, and solutions have been limited to assuming a constant depth of material in filter concentrates (Passow et al. 1994), or assessing only particle number and surface area and assuming spherical shapes (Mostajir et al. 1995a,b, Schumann & Rentsch 1998). Using the present method of concentrating plankton and detritus on a Nuclepore filter between a glass slide and coverslip, the range in thickness of individual detrital particles was about 1 order of magnitude. While filter concentration of detrital particles may have changed their original shape, the ability to optically section such concentrated samples (Verity et al. 1996) integrated this variability.

The complete protocol described here is rather tedious and time-consuming to routinely estimate C:V and N:V ratios in either cultured or natural communities. However, the methods used to collect, stain, preserve, and determine only the volume of detritus are much simpler and faster. Moreover, while a *z*-axis motorized microscope stage was used here, the same procedure of collecting stacks of 2D images can be accomplished manually if the microscope has an accurate calibrated fine focus. Once the 2D images are collected, the remainder of the procedure to determine detritus volume can be efficiently completed using commercial or custom image analysis software (e.g. Shopov et al. 2000). Thus, the major objective of this study was to determine C:V and N:V ratios for phytoplankton-derived detritus, so that carbon and nitrogen contents can be derived from the comparatively simple volume measurements.

Similarities and differences were apparent in the degradation of the 2 phytoplankton species in the dark. Bulk POC and PON in both cultures exhibited patterns of decline which could be modeled as first order decay constants (Figs. 2 & 7, Tables 1 & 3). The dual phase degradation model suggested that most of the POC and PON in the *Cryptomonas* sp. and *Gymnodinium* sp. cultures was rapidly leached or degraded, although bulk PON in the *Gymnodinium* sp. culture was apparently less labile. The less labile fractions were leached or degraded an order of magnitude slower than the more labile fractions. The rate constants predicted that the labile material in *Cryptomonas* sp. was leached or degraded faster than that in *Gymnodinium* sp., but that after 56 d more bulk POC and PON in the *Gymnodinium* sp. culture was lost than in the *Cryptomonas* sp. culture. The differences may reflect the composition of the particulate matter or the associated bacteria communities (discussed below). Accordingly, the single phase exponential model predicted shorter half-lives for bulk POC and PON in *Gymnodinium* sp. compared to *Cryptomonas* sp. Note that these experiments were not designed to create

carbon/nitrogen budgets; hence dissolved pool sizes and respiration were not measured.

The C:N ratios of bulk particulate matter increased over the 8 wk incubation, indicating more rapid losses of PON compared to POC; this was especially true of *Gymnodinium* sp. In addition to losing more nitrogen relative to carbon compared to *Cryptomonas* sp., the cellular chl *a* content of *Gymnodinium* sp. also degraded more rapidly. However, while the initial C:chl and N:chl ratios of *Cryptomonas* sp. were 6 to 7 times lower than *Gymnodinium* sp., the chl *a* of *Cryptomonas* sp. was more resistant to degradation. Ultimately the POC, PON, chl *a* contents and their respective ratios converged for both species.

The organisms apparently responsible for this dark-mediated degradation were the associated bacterial communities. In both experiments, the maximum abundance and biomass of bacteria were similar, i.e. 2.7 to 3.1×10^8 cells ml^{-1} and 2.5 to 3.0 mg C l^{-1} (Figs. 4 & 9). This would convert to an approximate mean biomass of 10 fg C $cell^{-1}$, which is similar to that for slow-growing natural bacteria (12 fg C $cell^{-1}$: Fukuda et al. 1998). The 2 bacterial communities in the present study certainly qualify as slow-growing. In the *Cryptomonas* sp. culture, the net increase of total bacteria was 3-fold over 57 d, with most of the growth in the first 2 wk; in *Gymnodinium* sp., no significant increases in abundance occurred, and a 3-fold decline occurred over the last weeks. While cultured bacteria are generally larger than natural bacteria, the former are also thought to be less dense than natural cells (Kirchman 2000).

Interestingly, bacterial communities in the 2 algal cultures exhibited different patterns in the proportions of metabolically active cells. The method used here combines rRNA targeted oligonucleotide probes, the general cell stain DAPI, and the membrane integrity stain propidium iodide, to quantitatively identify cells with compromised membranes and those cells containing sufficient rRNA to be considered metabolically active. This VSP (Vital Stain and Probe) technique differentiates cell physiological status based on 2 independent cellular criteria: membrane integrity and cellular rRNA content. Using this method it is possible to distinguish between 4 physiologically distinct cell types: (1) cells that are dead but were recently active (<24 to 36 h), (2) cells that are dead, (3) cells that are living and active, and (4) cells that are inactive but not dead (Williams et al. 1998, Howard-Jones et al. in press). This protocol has also been used to examine the physiological status of microbial communities in a variety of planktonic marine environments with respect to various biological, chemical, and physical parameters (Williams et al. 1999).

In *Cryptomonas* sp., the active fraction was typically high (80 to 90%) during the first 5 wk, and only decreased to 60–70% during the last 3 wk (Fig. 4). In *Gymnodinium* sp., the active fraction was initially much lower (25%) and decreased steadily after the third week (Fig. 9). Whether these differences reflected differences in bacterial community composition between the 2 cultures, the composition of the particulate matter, and/or substrate limitation is unknown. Both bacterial communities contained relatively few dead cells. The strong inverse relationships between the fraction of active bacteria and the C:N ratio of the total POM suggest that the microbial communities in these cultures responded to availability of nitrogen (and perhaps other nutrients) in either the particulate or dissolved fractions. Similarly, activity *in situ* was found to be positively correlated with proxies for either phytoplankton productivity or substrate availability (Williams et al. 1999). Note that the present experiments were not designed to, and do not distinguish between, limitation of bacteria growth or POM degradation due to dissolved versus particulate resource availability, or to distinguish limitation by resources other than carbon or nitrogen. Bacterial communities associated with phytoplankton cultures may not resemble those *in situ*, e.g. cultures are likely much lower in taxonomic diversity, although their roles remain similar. It can therefore be argued that degradation rates reported here may not be representative of natural communities. However, it is also instructive to note that the range in apparent metabolic activity of bacteria cells in the present cultures is similar to that reported from a variety of estuarine, coastal, and oligotrophic waters (Kemp et al. 1993, del Giorgio & Scarborough 1995, Choi et al. 1996, Karner & Fuhrman 1997, Gasol et al. 1999, Sherr et al. 2000). Moreover, the inverse relationship between substrate C:N ratios and the active bacteria fraction observed here agrees with similar inverse relationships reported between substrate C:N ratios and bacteria growth yield, e.g. Linley & Newell (1984).

The different rates of decay of the 2 phytoplankton species induced different patterns in accumulation of bacterial biomass. *Cryptomonas* sp. POC did not disappear until Day 39, and the fraction of total POC represented by bacteria increased steadily until that time, after which it declined (Fig. 5). *Gymnodinium* sp. POC disappeared by Day 28, and the fraction of total POC represented by bacteria declined after that date (Fig. 10). At the time of their peak contributions, bacteria represented 55 to 72% of total POC in the cultures but only 13 to 17% of the total initial POC. The bacteria conversion efficiencies in terms of carbon (Linley & Newell 1984: bacteria carbon produced/algal carbon degraded) were 7.9% (*Gymnodinium* sp.) and 9.2% (*Cryptomonas* sp.). Patterns in the proportion of total PON represented by bacteria were similar to those of

POC, with one important exception: the magnitudes were much greater. Bacteria in both cultures conserved nitrogen compared to carbon. At their peaks (Week 8 for *Cryptomonas* sp., Week 4 for *Gymnodinium* sp.), bacteria represented 85 to 90% of the bulk PON remaining in each culture, but only 15 to 19% of total initial PON. The bacteria conversion efficiencies in terms of nitrogen were 10.2% (*Cryptomonas* sp.) and 11.1% (*Gymnodinium* sp.). The carbon conversion efficiencies are at the lower end of the range of 10 to 20% often reported for similar incubation studies (Newell et al. 1981, Linley & Newell 1984, Pomeroy et al. 1984, Osinga et al. 1997). Note that these efficiencies are conservative to the extent that unaccounted loss processes, e.g. viral lysis, were significant.

The initial C:V and N:V ratios of detritus derived from *Cryptomonas* sp. and *Gymnodinium* sp. were similar, ranging from 0.09 to 0.11 and 0.02 to 0.03, respectively (Tables 2 & 4). Thereafter, patterns of the 2 taxa diverged. C:V and N:V ratios of detritus derived from *Cryptomonas* sp. declined 5- to 6-fold and 7- to 9-fold, respectively, over the next 5 wk. In contrast, mass:volume ratios in *Gymnodinium* sp. were relatively constant at 0.010 to 0.011 and 0.003 to 0.004. The explanation for this difference is not readily apparent, but may reflect the much higher C:N ratios of the bulk matter in the *Gymnodinium* sp. culture compared to *Cryptomonas* sp. Degradation rates are known to vary considerably among phytoplankton taxa according to their biochemical composition and cell wall constituents (Gunnison & Alexander 1975, Newell et al. 1981, Linley & Newell 1984, Biddanda 1988). The greater losses of carbon and nitrogen relative to volume of detritus in the *Cryptomonas* sp. culture may also be related to the considerably higher percentages of active bacteria cells there.

Interestingly, the magnitude and temporal trends in the C:N ratios of detritus derived from the 2 phytoplankton taxa were comparatively similar. Detritus in both cultures exhibited initial values of 27 to 30, increased to 44–53 after 5 wk of degradation, and then declined to ratios more similar to initial values. Initially, detrital C:N ratios were considerably higher than bulk C:N ratios in both cultures. In the *Cryptomonas* sp. culture, detrital C:N ratios remained typically 3 to 4 times higher than bulk C:N ratios, because approximately equal portions of bulk PON were in the form of bacteria and detritus in the later stages of degradation (Fig. 6). In the *Gymnodinium* sp. culture, where most of the PON was in the form of bacteria late in degradation (Fig. 11), bulk C:N ratios were more similar to detrital C:N ratios. In both cultures, the high C:N ratios of detritus may reflect both preferential conservation of nitrogen by bacteria and accumulation of exopolymer carbon from dissolved organic matter (Alber & Valiela 1994, Mari & Burd 1998). On the date with peak detritus concentrations in the *Cryptomonas* sp. culture, detritus yields (detritus produced/algal degraded) were 15.9 and 2.3% for carbon and nitrogen, respectively. After 56 d, these yields were 11.2 and 1.0%. For *Gymnodinium* sp., detritus yields at peak detritus concentrations were 13.7 and 3.4% for carbon and nitrogen, respectively. After 56 d, these yields were 10.8 and 2.2%. Thus, relatively similar detrital carbon yields (11 to 16%) and nitrogen yields (1 to 3%) were found. Since the bacteria yields were 8 to 9% (carbon) and 10 to 11% (nitrogen), most of the algal biomass was converted to dissolved organic and inorganic forms.

The C:V and N:V ratios of detritus in our cultures are lower, and the C:N ratios of detritus are higher, than the limited data estimated from a natural shelf plankton community (Verity et al. 1996), where mean C:V and N:V ratios were 0.23 and 0.011 pg μm^{-3}, or 2 to 4 times and 3 to 8 times higher, respectively, than mean ratios in detritus from decaying phytoplankton cultures. The field C:N ratios ranged from 6 to 44, with a mean of 21, compared to the cultures, which ranged from 23 to 53, with an overall mean of 37. However, the discrepancies are smaller when field data are compared to 'young' detritus from our cultures, which had C:V and N:V ratios of 0.1 and 0.003, respectively, and C:N ratios of 27 to 30 (Tables 2 & 4). This suggests that bulk detritus in the mixed layer of a moderately productive shelf ecosystem may be biochemically younger than detritus derived from senescent phytoplankton cultures, and therefore it contains more elemental mass per unit volume than cultures. Alternatively or additionally, other processes may operate *in situ* which enrich detrital density. Detritus from other natural plankton communities also has higher C:V and N:V ratios, and lower C:N ratios, than those estimated for these cultures, supporting one or more of these hypotheses (Verity et al. unpubl.). Given the degradation rates measured here, which are similar to those in other phytoplankton cultures (Newell et al. 1981, Biddanda 1988, Pett 1989, Osinga et al. 1997), the elementally rich ratios found in natural communities imply substantial and continuous production of fresh detritus within the mixed layer. In the lab, this hypothesis could be tested by using similar incubations but with bacterivores present to regenerate nutrients and thereby stimulate more rapid degradation, and by using multiple senescent phytoplankton. Similar incubations using mixed natural communities may also prove instructive, although grazer-mediated formation and ingestion of detritus may complicate interpretation of patterns.

The mass:volume ratios of detritus can also be compared to those of living plankton. Eucaryotic photosynthetic nanoplankton, treated with the same preserva-

tives and measured using similar image analysis techniques, had carbon densities of 0.13 to 0.31 pg C μm^{-3} and nitrogen densities of 0.017 to 0.047 pg N μm^{-3} (Verity et al. 1992). Similarly sized heterotrophic nanoplankton contained 0.18 to 0.30 pg C μm^{-3} (Fenchel 1982, Borsheim & Bratbak 1987). Smaller procaryotic phytoplankton contained 0.15 to 0.47 pg C μm^{-3} (Stramski & Morel 1990, Verity et al. 1992). Even smaller bacteria have typical carbon densities of 0.38 to 0.72 pg C μm^{-3} (Bratbak 1985, Lee & Fuhrman 1987, Kroer 1994), although lower values have been also reported (Nagata 1986, Norland et al. 1987, Nagata & Watanabe 1990). In contrast, larger ciliate microplankton have lower carbon densities of 0.09 to 0.19 pg C μm^{-3} (Heinbokel 1978, Putt & Stoecker 1989). Thus, evidence indicates that both within trophic levels (phytoplankton: Verity et al. 1992, Montagnes et al. 1994 and citations therein; bacteria: Norland et al. 1987, Simon & Azam 1989) and across unicellular plankton trophic levels, mass:volume ratios are inversely related to cell size. As would be predicted, the mass:volume ratios of detritus are less than those of living plankton, especially nitrogen. However, given that plankton cell quotas vary with physiological state (e.g. Thompson et al. 1991), and that natural detritus is derived from organisms of many sizes (and physiological states), mass:volume of detritus *in situ* may vary considerably.

Acknowledgements. This research benefited from the contributions of numerous individuals. C. Y. Robertson ran numerous CHN samples and taught others how to do so. The original VSP method was developed by many people (Williams et al. 1998), and would not have been possible without the early work and ideas of M. E. Frischer. The development of the image analysis system was possible because of the foresight of the Skidaway Institute of Oceanography, at that time directed by D. W. Menzel, and the support of the US National Science Foundation and the Department of Energy during the past decade. In particular, this research was funded by NSF grants OCE-95-21086 and 96-17884. D. Peterson ably drafted the manuscript, and S. Macintosh and A. Boyette styled the figures.

LITERATURE CITED

Alber M, Valiela I (1994) Biochemical composition of organic aggregates produced from marine macrophyte-derived organic matter. Limnol Oceanogr 39:717–723

Alldredge A (1998) The carbon, nitrogen, and mass content of marine snow as a function of aggregate size. Deep-Sea Res I 45:529–541

Alldredge AL, Passow U, Logan BE (1993) The abundance and significance of a class of large, transparent organic particles in the ocean. Deep-Sea Res 40:1131–1140

Amann RI, Ludwig W, Schleifer KH (1995) Phylogenetic identification and *in situ* detection of individual microbial cells without cultivation. Microbiol Rev 59:143–169

Anderson TR, Williams PJLeB (1998) Modeling the seasonal cycle of dissolved organic carbon at Station E1 in the English Channel. Estuar Coast Shelf Sci 46:93–109

Andersson A, Rudehall A (1993) Proportion of plankton biomass in particulate organic carbon in the northern Baltic Sea. Mar Ecol Prog Ser 95:133–139

Banse K (1977) Determining the carbon-to-chlorophyll ratio of natural phytoplankton. Mar Biol 41:199–212

Berner RA (1980) Early diagenesis: a theoretical approach. Princeton University Press, Princeton

Biddanda BA (1988) Microbial aggregation and degradation of phytoplankton-derived detritus in seawater. II. Microbial metabolism. Mar Ecol Prog Ser 42:89–95

Biddanda BA, Pomeroy LR (1988) Microbial aggregation and degradation of phytoplankton-derived detritus in seawater. I. Microbial succession. Mar Ecol Prog Ser 42:79–88

Bode A, Figueroa FL, Ruiz J (1994) Estimating the photosynthetic and detrital fractions of seston: a comparison of methods. Working group 5 report. Sci Mar 58:59–65

Borsheim KY, Bratbak G (1987) Cell volume to cell carbon conversion factors for a bacterivorous *Monas* sp. enriched from seawater. Mar Ecol Prog Ser 36:171–175

Bratbak G (1985) Bacterial biovolume and biomass estimations. Appl Environ Microbiol 49:1488–1493

Braun-Howland EB, Danielsen SA, Nierzwicki-Bauer SA (1992) Development of a rapid method for detecting bacterial cells *in situ* using 16S rRNA-targeted probes. Biotechniques 13:928–934

Choi JW, Sherr EB, Sherr BF (1996) Relation between presence-absence of a visible nucleoid and metabolic activity in bacterioplankton cells. Limnol Oceanogr 41:1161–1168

Decho AW (1990) Microbial exopolymer secretions in ocean environments: their role(s) in food webs and marine processes. Oceanogr Mar Biol Annu Rev 28:73–153

del Giorgio PA, Scarborough G (1995) Increase in the proportion of metabolically active bacteria along gradients of enrichment in freshwater and marine plankton: implications for estimates of bacterial growth and production. J Plankton Res 17:1905–1924

Fenchel T (1982) Ecology of heterotrophic microflagellates. II. Bioenergetics and growth. Mar Ecol Prog Ser 8:225–231

Fukuda R, Ogawa H, Nagata T, Koike I (1998) Direct determination of carbon and nitrogen contents of natural bacterial assemblages in marine environments. Appl Environ Microbiol 64:3352–3358

Gasol JM, Zweifel UL, Peters F, Fuhrman JA, Hagström Å (1999) Significance of size and nucleic acid content heterogeneity as measured by flow cytometry in natural planktonic bacteria. Appl Environ Microbiol 65: 4475–4483

Gassmann G, Gillbricht M (1982) Correlations between phytoplankton, organic detritus, and carbon in North Sea waters during the Fladenground Experiment (FLEX '76). Helgol Meeresunters 35:253–262

Giovannoni SJ, DeLong EF, Olsen GJ, Pace NR (1988) Phylogenetic group-specific oligodeoxynucleotide probes for identification of single microbial cells. J Bacteriol 170: 720–726

Gordon DC Jr (1970) A microscopic study of organic particles in the North Atlantic Ocean. Deep-Sea Res 17:175–185

Guillard RRL (1975) Culture of phytoplankton for feeding marine invertebrates. In: Smith WL, Chanley MH (eds) Culture of marine invertebrate animals. Plenum, New York, p 29–60

Gunnison D, Alexander M (1975) Resistance and susceptibility of algae to decomposition by natural microbial communities. Limnol Oceanogr 20:64–70

Heinbokel JF (1978) Studies on the functional role of tintinnids in the Southern California Bight. I. Grazing and growth rates in laboratory cultures. Mar Biol 47:177–189

Hong Y, Frischer ME, Verity PG, Danforth J (1998) *In vivo* rRNA degradation rates: identification of dead but recently active cells in marine microbial communities. 98th General Meeting of the American Society for Microbiology, Atlanta, GA, USA. American Society for Microbiology, Washington, DC

Howard-Jones MH, Frischer ME, Verity PG (in press) Determining the physiological status of individual bacteria cells. In: Paul JH (ed) Methods in microbiology, Vol 30. Academic Press, New York

Kane JE (1967) Organic aggregates in surface waters of the Ligurian Sea. Limnol Oceanogr 12:287–294

Karner M, Fuhrman JA (1997) Determination of active marine bacterioplankton: a comparison of universal 16S rRNA probes, autoradiography, and nucleoid staining. Appl Environ Microbiol 63:1208–1213

Kemp PF, Lee S, LaRoche J (1993) Estimating growth rate of slowly growing marine bacteria from RNA content. Appl Environ Microbiol 59:2594–2601

Khaylov KM, Finenko ZZ (1968) Interaction of detritus with high-molecular-weight components of dissolved organic matter in seawater. Oceanology 8:776–785

Kirchman DL (2000) Uptake and regeneration of inorganic nutrients by marine heterotrophic bacteria. In: Kirchman DL (ed) Microbial ecology of the oceans. John Wiley and Sons, Inc, New York, p 261–288

Kroer N (1994) Relationships between biovolume and carbon and nitrogen content of bacterioplankton. FEMS Microbiol Ecol 13:217–224

Lane DJ, Pace B, Olsen GJ, Stahl DA, Sogin ML, Pace NR (1985) Rapid determination of 16S ribosomal RNA sequences for phylogenetic analyses. Proc Natl Acad Sci USA 82:6955–6959

Lee S, Fuhrman JA (1987) Relationships between biomass and biovolume of naturally derived marine bacterioplankton. Appl Environ Microbiol 53:1298–1303

Lee S, Malone C, Kemp PF (1993) Use of multiple 16S rRNA targeted fluorescent probes to increase signal strength and measure cellular RNA from natural planktonic bacteria. Mar Ecol Prog Ser 101:193–201

Linley EAS, Newell RC (1984) Estimates of bacterial growth yields based on plant detritus. Bull Mar Sci 35:409–425

Mari X, Burd A (1998) Seasonal size spectra of transparent exopolymeric particles (TEP) in a coastal sea and comparison with those predicted using coagulation theory. Mar Ecol Prog Ser 163:63–76

Montagnes DJS, Berges J, Harrison PJ, Taylor FJR (1994) Estimating carbon, nitrogen, protein, and chlorophyll a from volume in marine phytoplankton. Limnol Oceanogr 39:1044–1060

Mostajir B, Dolan JR, Rassoulzadegan F (1995a) A simple method for the quantification of a class of labile marine pico- and nano-sized detritus: DAPI Yellow Particles (DYP). Aquat Microb Ecol 9:259–266

Mostajir B, Dolan JR, Rassoulzadegan F (1995b) Seasonal variations in pico- and nano-detrital particles (DAPI Yellow Particles, DYP) in the Ligurian Sea (NW Mediterranean). Aquat Microb Ecol 9:267–277

Nagata T (1986) Carbon and nitrogen content of natural planktonic bacteria. Appl Environ Microbiol 52:28–32

Nagata T, Watanabe Y (1990) Carbon- and nitrogen-to-volume ratios of bacterioplankton growth under different nutritional conditions. Appl Environ Microbiol 56: 1303–1309

Newell RC, Lucas MI, Linley EAS (1981) Rate of degradation and efficiency of conversion of phytoplankton debris by marine micro-organisms. Mar Ecol Prog Ser 6:123–136

Norland S, Heldal M, Tumyr O (1987) On the relation between dry matter and volume of bacteria. Microb Ecol 13:95–101

Osinga R, deVries K, Lewis WE, van Raaphorst W, Dijkhuizen L, van Duyl FC (1997) Aerobic degradation of phytoplankton debris dominated by *Phaeocystis* sp. in different physiological stages of growth. Aquat Microb Ecol 12:11–19

Otsuki A, Hanya T (1972) Production of dissolved organic matter from dead green algal cells. I. Aerobic decomposition. Limnol Oceanogr 17:248–257

Paerl HW (1974) Bacterial uptake of dissolved organic matter in relation to detrital aggregation in marine and freshwater systems. Limnol Oceanogr 19:966–972

Parsons TR, Maita Y, Lalli CM (1984) A manual of chemical and biological methods for seawater analysis. Pergamon Press, New York

Passow U, Alldredge AL (1994) Distribution, size, and bacterial colonization of transparent exopolymer particles (TEP) in the ocean. Mar Ecol Prog Ser 113:185–198

Passow U, Alldredge AL, Logan BE (1994) The role of particulate carbohydrate exudates in the flocculation of diatom blooms. Deep-Sea Res I 41:335–357

Pett RJ (1989) Kinetics of microbial mineralization of organic carbon from detrital *Skeletonema costatum* cells. Mar Ecol Prog Ser 52:123–128

Pomeroy LR (1979) Secondary production mechanisms of continental shelf communities. In: Livingston RJ (ed) Ecological processes in coastal and marine ecosystems. Plenum Press, New York, p 163–186

Pomeroy LR (1980) Detritus and its role as a food source. In: Barnes RK, Mann KH (eds) Fundamentals of aquatic ecosystems. Blackwell Sci. Publ, London, p 84–102

Pomeroy LR, Hanson RB, McGillivary PA, Sherr BF, Kirchman D, Deibel D (1984) Microbiology and chemistry of fecal products of pelagic tunicates: rates and fates. Bull Mar Sci 35:426–439

Putt M, Stoecker DK (1989) An experimentally determined carbon:volume ratio for marine 'oligotrichous' ciliates from estuarine and coastal waters. Limnol Oceanogr 34: 1097–1103

Rice DL (1982) The detritus nitrogen problem: new observations and perspectives from organic geochemistry. Mar Ecol Prog Ser 9:153–162

Roman M, Tenore KR (1984) Detritus dynamics in aquatic ecosystems: an overview. Bull Mar Sci 35:257–260

Schumann R, Rentsch D (1998) Staining particulate organic matter with DTAF — a fluorescent dye for carbohydrates and protein: a new approach and application of a 2D image analysis system. Mar Ecol Prog Ser 163:77–88

Sgorbati S, Barbesti S, Citterio S, Bestetti G, DeVecchi R (1996) Characterization of number, DNA content, viability and cell size of bacteria from natural environments using DAPI/PI dual staining and flow cytometry. Minerva Biotecnologica 8:9–15

Sherr EB, Sherr BF, Sigmon CT (2000) Activity of marine bacteria under incubated and *in situ* conditions. Aquat Microb Ecol 20:213–223

Shopov A, Williams SC, Verity PG (2000) Improvements in image analysis and fluorescence microscopy to discriminate and enumerate bacteria and viruses in aquatic samples. Aquat Microb Ecol 22:103–110

Sieracki ME, Reichenbach S, Webb KW (1989a) An evaluation of automated threshold detection methods for accurate sizing of microscopic fluorescent cells by image analysis. Appl Environ Microbiol 55:2762–2772

Sieracki ME, Viles CL, Webb KW (1989b) Algorithm to estimate cell biovolume using image analyzed microscopy. Cytometry 10:551–557

Simon M, Azam F (1989) Protein content and protein synthe-

sis rates of planktonic marine bacteria. Mar Ecol Prog Ser 51:201–213

Smetacek V (1980) Zooplankton standing stock, copepod fecal pellets and particulate detritus in Kiel Bight. Estuar Coast Mar Sci 11:477–490

Smetacek V, Hendricksen P (1979) Composition of particulate organic matter in Kiel Bight in relation to phytoplankton succession. Oceanol Acta 2:287–298

Stramski D, Morel A (1990) Optical properties of photosynthetic picoplankton in different physiological states as affected by growth irradiance. Deep-Sea Res 37:245–266

Thompson PA, Harrison PJ, Parslow JS (1991) Influence of irradiance on cell volume and carbon quota for ten species of marine phytoplankton. J Phycol 27:351–360

Verity PG (2000) Grazing experiments and model simulations of the role of zooplankton in *Phaeocystis* food webs. J Sea Res 43:317–343

Verity PG, Sieracki ME (1993) Use of color image analysis and epifluorescence microscopy to measure plankton biomass. In: Kemp PF, Sherr BF, Sherr EB, Cole JJ (eds) Handbook of methods in aquatic microbial ecology. Lewis Publ, London, p 327–338

Verity PG, Robertson CY, Tronzo CR, Andrews MG, Nelson JR, Sieracki ME (1992) Relationships between cell volume and the carbon and nitrogen content of marine photosynthetic nanoplankton. Limnol Oceanogr 37:1434–1446

Verity PG, Beatty TM, Williams SC (1996) Visualization and quantification of plankton and detritus using digital confocal microscopy. Aquat Microb Ecol 10:55–67

Vescio PA, Nierzwicki-Bauer SA (1995) Extraction and purification of PCR amplifiable DNA from lacustrine subsurface sediments. J Microbiol Methods 21:225–233

Williams SC, Verity PG, Beatty T (1995) A new staining technique for dual identification of plankton and detritus in seawater. J Plankton Res 17:2037–2047

Williams SC, Hong Y, Danavall DCA, Howard-Jones MH, Gibson D, Frischer ME, Verity PG (1998) Distinguishing between living and nonliving bacteria: evaluation of the vital stain propidium iodide and the combined use with molecular probes in aquatic samples. J Microbiol Methods 32:225–236

Williams SC, Alkaff H, Hong Y, Penill L, Shopov A, Frischer M, Verity PG (1999) Use of a combined vital stain and probe method to distinguish between metabolically active and inactive bacteria in the natural aquatic environment. Abstract N-99. American Society for Microbiology General Meeting, 1999, Chicago, IL. American Society for Microbiology, Washington, DC

Editorial responsibility: Otto Kinne (Editor), Oldendorf/Luhe, Germany

Submitted: February 21, 2000; Accepted: May 23, 2000
Proofs received from author(s): October 26, 2000